ACCSCIENCE PUBLISHING

Asian Journal of Water, Environment and Pollution

REVIEW ARTICLE

Quantum dots: A promising photocatalytic nanomaterial in water environment remediation

Shuan Liu[1]*, Yuhui Yang[1], Qixin Pan[2], Yinghao Xue[3], Weixuan Huang[4], Yunqian Song[5], and Xingpeng Wang[1]*

[1]Department of Environment and Engineering, College of Hydraulic and Architectural Engineering, Tarim University, Alaer, Xinjiang, China

[2]Department of Environmental Science and Engineering, College of Environment and Ecology, Chongqing University, Chongqing, China

[3]Department of Environmental Science and Engineering, College of Chemical Engineering, Beijing University of Chemical Technology, Beijing, China

[4]Faculty of Education and Liberal Arts, INTI International University, Nilai, Negeri Sembilan, Malaysia

[5]Australian Centre for Water and Environmental Biotechnology, The University of Queensland, Brisbane, Queensland, Australia

Abstract

Photocatalysis is a green and energy-efficient strategy to mitigate energy demand and control environmental pollution. Quantum dots (QDs) are a promising nanomaterial with excellent stability, relatively low toxicity, and superior photoelectric properties, which can significantly enhance the conversion efficiency of photocatalysts. This review introduces representative methods for preparing QDs, including hydrothermal, pyrolysis, ultrasonic, electrochemical stripping, and etching methods. The applicable conditions, strengths, and limitations of each synthetic technique are comprehensively discussed. In addition, the latest progress in QD-modifying photocatalysts for pollutant removal and hydrogen peroxide production is reviewed. Doping of QDs can optimize catalytic performance in multiple ways: broadening the visible light response range, facilitating carrier separation, accelerating electron migration, and tuning the band gap structure. Finally, we present the challenges and prospects of QD-modifying photocatalysts in the context of preparation, water environment remediation, and energy conversion. Overall, this review aims to provide novel insights into QD-modifying photocatalysts in remediating water pollution and alleviating energy crises.

Keywords: Quantum dots; Photocatalysis; Pollutant removal; Hydrogen peroxide production

***Corresponding authors:**
Shuan Liu
(liushuan159@163.com);
Xingpeng Wang
(13999068354@163.com)

Citation: Liu S, Yang Y, Pan O, *et al*. Quantum dots: A promising photocatalytic nanomaterial in water environment remediation. *Asian J Water Environ Pollut*. 2026;23(5):026240167. doi: 10.36922/AJWEP026240167

Received: June 10, 2026

Revised: June 16, 2026

Accepted: June 18, 2026

Published online: August 28, 2026

Copyright: © 2026 Author(s). This is an Open-Access article distributed under the terms of the Creative Commons Attribution License, permitting distribution, and reproduction in any medium, provided the original work is properly cited.

Publisher's Note: AccScience Publishing remains neutral with regard to jurisdictional claims in published maps and institutional affiliations.

1. Introduction

Global energy demand has surged rapidly over the past few decades. The over-reliance on fossil fuels has simultaneously triggered severe energy shortages and widespread water pollution.[1] Meanwhile, the arbitrary discharge of wastewater from industries such as printing and dyeing, textiles, and pharmaceuticals has caused serious pollution of the water environment. Fortunately, photocatalytic technology can be applied to hydrogen peroxide (H_2O_2) production and pollutant removal to alleviate water environmental

pollution and the energy crisis.[2,3] Upon light irradiation, semiconductors absorb photon energy, enabling electrons to jump from the valence band (VB) to the conduction band (CB) and form electron-hole pairs. The photogenerated holes on VB react with adsorbed water molecules (H_2O) to produce $^{\bullet}OH$, which can oxidize organic contaminants.[4] The electrons on CB can reduce oxygen (O_2) to form $O_2^{\bullet-}$ and H_2O_2, and these electrons can also drive water splitting to generate hydrogen gas.[5,6] However, conventional titanium oxide (TiO_2) and graphitic carbon nitride (g-C_3N_4) face the dilemma of a narrow light absorption range and low photogenerated charge carrier separation efficiency.[7]

Quantum dots (QDs) are zero-dimensional nanocrystals whose overall size is smaller than the exciton Bohr radius in three dimensions.[8] Generally, their particle size ranges from 2 nm to 10 nm, which limits the movement of internal electrons.[9-11] Compared to traditional bulk semiconductors, the bandgap of QDs can be precisely adjusted by size to obtain a more suitable range of light absorption, which is conducive to improving photocatalytic conversion efficiency.[12] Further, owing to the ultrasmall size of QDs, the photogenerated charge is transferred from the interior of the QDs to the catalyst surface over a short distance, facilitating the rapid transport and separation of photogenerated excitons.[13] Therefore, various types of QDs, such as carbon (C) QDs (CQDs), graphene carbon (G) QDs (GQDs), carbon nitride (CN) QDs (CNQDs), black phosphorus (BP) QDs (BPQDs), MXene QDs (MQDs), and metal compound (MC) QDs (MCQDs), are currently thriving in fields of photocatalysis.[9-11]

Quantum dots are often used to modify semiconductors, thereby improving the energy conversion efficiency of photocatalytic systems.[11-13] Raziq *et al.*[14] prepared P-doped g-C_3N_4 modified with cadmium selenide (CdSe) QDs (4CdSe/P-CN). The structural coupling between P-doping and CdSe QDs considerably expanded the light response range of the original g-C_3N_4 to 700 nm. Furthermore, 4CdSe/P-CN exhibited enhanced electron–hole separation efficiency. Moreover, photocatalysis is widely considered a low-carbon, efficient method for activating peroxymonosulfate (PMS).[15,16] Photogenerated electrons can trigger the activation of PMS, yielding $SO_4^{\bullet-}$ that are capable of degrading organic compounds. Ming *et al.*[17] fabricated CQD/g-C_3N_4 and verified its excellent performance toward PMS activation for BPA elimination. The TOC removal rate for BPA reached 77% within 30 min, which is much higher than the 23% achieved in the undoped process. This is because doping CQDs increased the specific surface area, light absorption, and charge separation of C_3N_4, properties favorable for PMS activation.

Quantum dots are playing an increasingly crucial role in the environment and energy sectors as nanotechnology advances. Therefore, it is necessary to comprehensively review the latest advances of QDs to guide future work. Several reviews of QDs have been conducted.[18-23] However, most of the reported reviews focused on only a single type of QDs or a single application of QD-modifying photocatalysts. Some researchers reviewed the coupling of CQDs/GQDs with traditional photocatalysts to remove pollutants from water.[18-20] In this review, we analyze the key synthesis methods for QDs and their advantages and disadvantages. Moreover, the latest advances in the application of QD-modifying photocatalysts for pollutant removal and H_2O_2 production are discussed in detail. Finally, we present the prospects for current challenges in the preparation and application of the water environment and energy. The summary of QD photocatalysts in this paper may not be exhaustive. However, this review provides insights into future research.

2. Preparation methods of quantum dots

Synthesis methods for QDs are crucial to their performance. The particle size, shape, and internal structure of QDs can be well tailored by optimizing preparation protocols and experimental conditions, thereby achieving targeted material performance.[23] In recent years, with advances in technology, diverse approaches have been developed to fabricate various QD types, including CQDs, GQDs, CNQDs, BPQDs, MQDs, and MCQDs. The synthesis strategies of QDs can be categorized into top-down and bottom-up methods. In this section, we discuss several mainstream QD fabrication methods and summarize their strengths and weaknesses in Table 1.

2.1. Top-down methods

The top-down method involves obtaining QDs by cleaving large, two- or three-dimensional precursors to nanoscale sizes via chemical or physical processes, including chemical etching, laser etching, electrochemical exfoliation, and ultrasonic methods. This type of method possesses the strengths of high efficiency and large-scale production. However, the top-down process may require expensive instrumentation and harsh experimental conditions. Moreover, achieving precise control over the size and morphology of QDs using this method proves challenging.

2.1.1. Chemical etching method

The chemical etching method involves oxidizing the source materials (graphite, carbon fibers, and MXenes) to obtain QDs. Peng *et al.*[24] prepared GQDs with different particle sizes (1–4 nm) by chemically treating carbon fibers with sulfuric acid/nitric acid to strip the stacked graphite from the fibers. Moreover, GQDs with different sizes and

fluorescent colors can be obtained by adjusting the reaction temperature. Li *et al.*[25] prepared MQDs by etching titanium carbide (Ti_3C_2) powder (Figure 1A). They dispersed 2 g of Ti_3C_2 powder in the hydrofluoric acid solution and stirred the mixture for 64 h. Dimethyl sulfoxide (10 mL) was added to the mixture, which was centrifuged at 3,600 rpm for 10 min. Subsequently, 3 mL of polyethyleneimine was added to the suspension, and the mixture was heated at 120 °C under a nitrogen gas (N_2) atmosphere. Ti_3C_2 QDs were synthesized via dialysis for seven days. Transmission electron microscopy (TEM) characterization revealed the microstructure and composition of the g-C_3N_4@Ti_3C_2 QD composites (Figure 1B and 1C). The lattice spacing of 0.26 nm corresponded to the (0110) plane of Ti_3C_2 QDs (Figure 1D). Elemental mapping (Figure 1E) further confirmed the uniform distribution of the C, nitrogen (N), and titanium (Ti) elements in the g-C_3N_4@Ti_3C_2 QD composites. The Ti_3C_2 QDs on the g-C_3N_4 surface act as an electron acceptor to promote the separation of photoexcited carriers.

As one of the earliest methods for synthesizing QDs, chemical etching offers the advantages of large-scale production and high selectivity. However, there are substantial drawbacks as well. The production process is time-consuming and requires complex post-processing steps, including centrifugation, neutralization, and dialysis. The use of acidic reagents may cause environmental pollution.

2.1.2. Ultrasonic method

Different from chemical etching methods, the ultrasonic method uses ultrasound-induced shock waves and cavitation to break the material into QDs.[26] Luo *et al.*[27] obtained GQDs using a dialysis bag after ultrasonic treatment of graphite in mixed acid. The GQDs prepared using this method had good crystallization with an average size of 2.5 nm. Chen *et al.*[28] first transferred 50 mg of BP powder into 100 mL of N-methylpyrrolidone as an intercalating agent (Figure 1F). Then, an ultrasonic instrument was used to sonicate the mixture at 600 W for 8 h to obtain a BP dispersion. N_2 was introduced into the

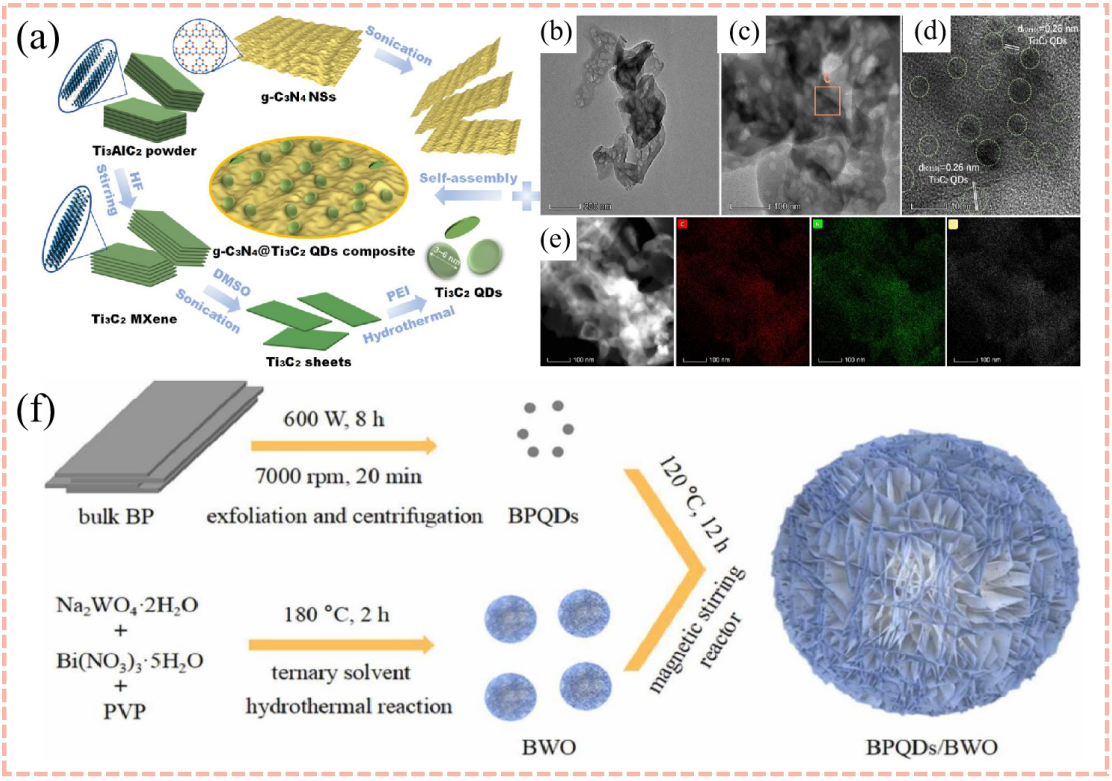

Figure 1. Schematic diagram of different QD synthesis methods. (A) The synthesis route of g-C_3N_4@Ti_3C_2. (B, C) TEM. Scale bars: 200 nm, 100 nm, 10 nm. (D) High-resolution TEM. Scale bar: 100 nm. (E) Energy-dispersive X-ray spectroscopy of g-C_3N_4@Ti_3C_2 QDs. Reprinted with permission from Li *et al.*[25] Copyright © 2019 American Chemical Society. (F) The synthesis route of BPQDs/BWO. Reprinted with permission from Chen *et al.*[28] Copyright © 2023 Elsevier.

Abbreviations: BP: Black phosphorus; BWO: Bismuth tungstate; DMSO: Dimethyl sulfoxide; g-C_3N_4: Graphitic carbon nitride; HF: Hydrofluoric acid; PEI: Polyethylenimine; PVP: Polyvinylpyrrolidone; QD: Quantum dot; TEM: Transmission electron microscopy; Ti_3C_2: Titanium carbide.

stripping process, and the temperature was maintained at 2 °C. The stripped BP suspension was centrifuged at 7,000 rpm for 20 min, and the supernatant containing BPQDs was collected. The ultrasonic method has the advantages of a short cycle, easy availability of raw materials, and low experimental cost.[26]

2.1.3. Electrochemical stripping method

Electrochemical stripping is another common method for synthesizing CQDs, with graphite rods usually used as anodes.[29] Under the application of anode voltage, H_2O is oxidized to generate $^{\bullet}OH$, which oxidatively decomposes the graphite rod.[30] Subsequently, the anion in the electrolyte further enters the graphite anode and acts as an intercalant, causing the graphite anode to expand. The expanded graphite is further oxidized and cleaved into very small graphene fragments. Finally, the graphene fragments are reduced and purified to obtain CQDs with high stability. Zhang *et al.*[29] inserted two graphite rods into an electrolyte solution in a beaker. One rod was designated the cathode, and the other, the anode. The mixture was stirred continuously for 120 h under a 30 V direct current power supply. The solution was dried at 80 °C to obtain black powder carbon dots. Afterward, ammonia was mixed with the powdered carbon dots and heated in a reactor at 150 °C for 7 h. Finally, the resulting mixture was centrifuged and dried to obtain CQD powder. This method can also be used to prepare GQDs, and the reaction mechanism is similar.[31]

These top-down methods possess the strengths of high efficiency and large-scale production. However, the top-down process may require expensive instrumentation and harsh experimental conditions. Moreover, achieving precise control over the size and morphology of QDs using this method proves challenging.

2.2. Bottom-up methods

Common bottom-up methods include the hydrothermal, pyrolysis, and microwave-assisted methods. The bottom-up method can quickly synthesize a large number of homogeneous QDs. Furthermore, this strategy enables fine regulation over the morphology and chemical characteristics of QDs while attaining a higher utilization rate of raw precursors.

2.2.1. Pyrolysis method

The pyrolysis method involves heating a carbon source in an atmosphere of inert gas at atmospheric pressure to obtain QDs. Dong *et al.*[32] synthesized blue-fluorescent GQDs by pyrolysis using citric acid as a carbon source. The obtained GQDs had a width of approximately 15 nm and a thickness of 0.5–2.0 nm. Ma *et al.*[33] mixed 1.01 g of melamine and 0.81 g of sodium citrate and ground them into a fine powder. Subsequently, they heated the mixed powder at 180 °C for 2 h. Finally, they washed these solids three times with ultrapure water and ethanol and dialyzed them with pure water for 24 h to obtain the CNQDs. The pyrolysis method possesses the strengths of simplicity and large-scale production. However, the size and morphology of the obtained QDs may be difficult to control.

2.2.2. Hydrothermal method

The method involves using organic precursor solutions as source material, sealing them in a hydrothermal reactor, and synthesizing QDs through high-pressure reactions. Currently, this method allows the use of various raw materials, such as citric acid, protein, boric acid, and lignin, as precursors for synthesizing CQDs.[34-36] For example, Li *et al.*[34] synthesized boron nitride (BN) QDs using the hydrothermal method (Figure 2A). They mixed 0.100 g of boric acid and 0.034 g of melamine and dissolved them in 10 mL of ultrapure water. After stirring for 30 min, the suspension was transferred into a hydrothermal reactor at 200 °C. The BNQDs were collected by filtration using a 0.22 μm ultrafiltration membrane. Scanning electron microscopy and TEM characterization showed that BNQDs were spherical with a diameter of approximately 3 nm (Figure 2B). Element mapping showed that the photocatalyst was mainly composed of the C, N, phosphorus (P), and boron (B) elements (Figure 2C). In addition, high-resolution TEM images showed that BNQDs exhibited a distinct lattice spacing of 0.21 nm, which was consistent with the (100) hexagonal pattern of boron nitride (Figure 2D). Qu *et al.*[35] synthesized N, sulfur (S)-CQDs from L-cysteine using the hydrothermal method. They used nitric acid as a carbonizing agent and ethylene glycol as a passivating agent (Figure 2E).

The hydrothermal method possesses the strengths of simple operation and controllable conditions. Moreover, the size, morphology, crystallinity, and properties of the QDs can be accurately controlled by adjusting the experimental conditions (e.g., reaction temperature, time, solvent, and precursor).[37] However, the hydrothermal method heats the reactants through thermal conduction and convection, thus requiring high temperatures and long reaction times. Furthermore, the high-pressure conditions during the experiment may pose a risk to safe production.

2.2.3. Microwave heating method

Microwave heating is an important method for material preparation. After absorbing microwaves, the dielectric material can convert electromagnetic energy into internal energy.[38] Ding *et al.*[39] dissolved p-phenylenediamine in ethylenediamine and placed the mixture in a microwave at

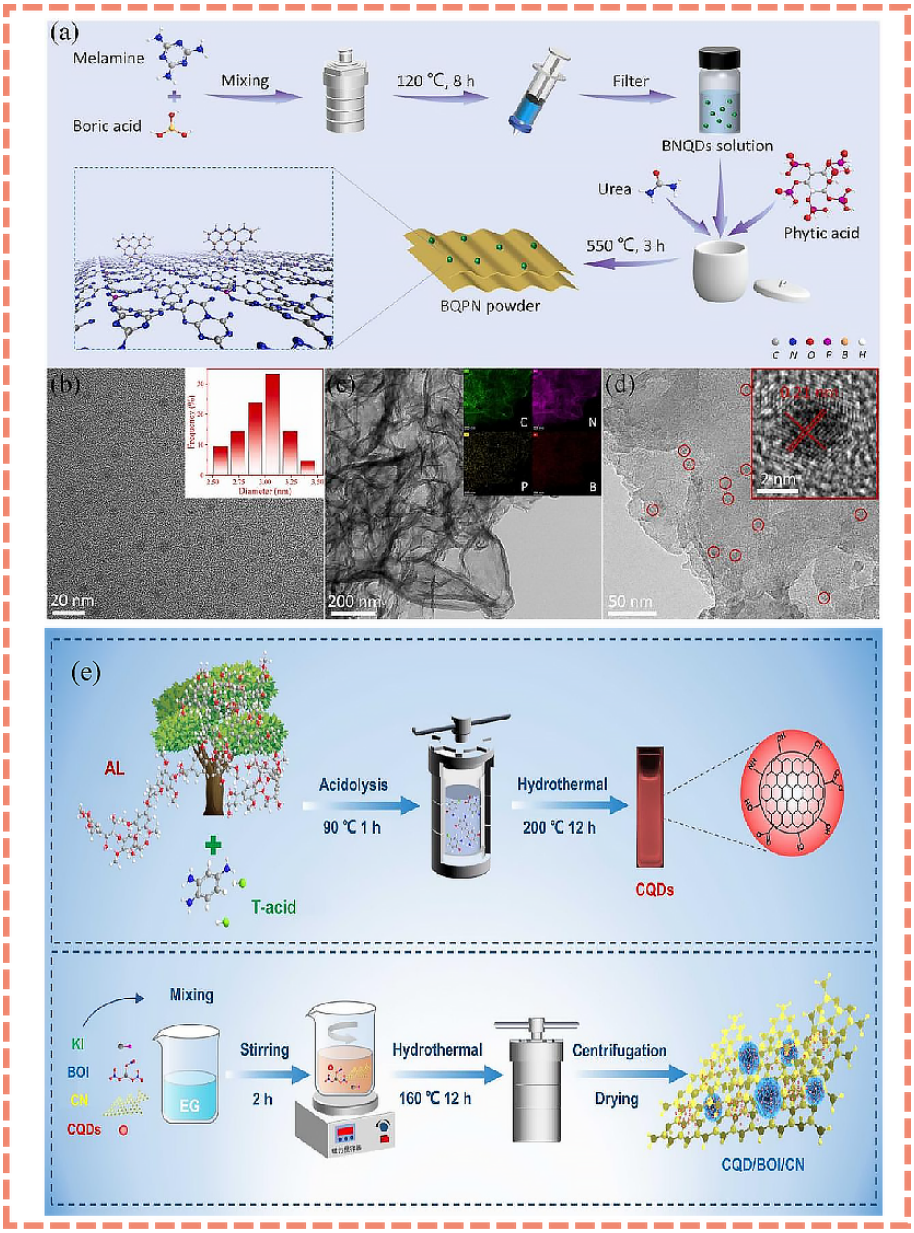

Figure 2. Schematic diagram of QD preparation and characterization. (A) The synthesis route for the preparation of BQPN. (B) TEM image of BNQDs. Scale bar: 20 nm. (C, D) TEM image of BQPN. Scale bars: 200 nm, 50 nm. Reprinted with permission from Li *et al.*[34] Copyright © 2022 Elsevier. (E) The synthesis route of CQD/BOI/CN. Reprinted with permission from Zhu *et al.*[36] Copyright © 2023 Elsevier.
Abbreviations: BNQD: Boron nitride quantum dot; BOI/CN: $Bi_7O_9I_3$/g-C_3N_4; BQPN: Boron nitride quantum dots modified P-doped g-C_3N_4 photocatalyst; CQD: Carbon quantum dot; QD: Quantum dot; TEM: Transmission electron microscope.

500 W for 20 min to prepare CQDs. Tang *et al.*[40] prepared GQDs from glucose via microwave-assisted hydrothermal synthesis. The prepared GQDs exhibited good crystallinity, with a size of 1.65 nm.

The raw materials used in the microwave method are mostly small organic molecules and biomass, similar to those used in the hydrothermal method. The microwave heating method can shorten reaction time to a few minutes, greatly reduce experimental costs, and avoid hazardous conditions such as high temperature and high pressure. Currently, this method is primarily used for the synthesis of CQDs/GQDs, and its application to the preparation of other QDs remains to be developed.

In summary, different QD preparation methods have

Table 1. Comparison of reported representative preparation methods of QDs

Type of QDs	Synthesis method	Merits	Demerits	Ref.
GQDs; MQDs	Chemical oxidation	Large-scale production and high selectivity	Time-consuming, complex post-processing, non-uniform size and morphology, and use of hazardous chemicals	24,25
GQDs; BPQDs	Ultrasound	Easy availability of raw materials, easy operation, and safe production	Low yield, instrumental wastage, and high energy cost	26-28
CQDs; GQDs	Electrochemical oxidation	Easy operation, safe production, uniform size and morphology, and good reproducibility	Low yield	29-31
GQDs; CNQDs	Pyrolysis	Solvent-free, low-cost, and large-scale production	Non-uniform size and morphology	32,33
BNQDs; N, S-CQDs	Hydrothermal	Simple operation and good reproducibility	High temperature, pressure, and time-consuming	34-36
CQDs; GQDs	Microwave heating	Short reaction time, uniform size and morphology, and good reproducibility	Limited application scope	38-40

Abbreviations: BN: Boron nitride; BP: Black phosphorus; C: Carbon; CN: Carbon nitride; G: Graphene carbon; M: Mxene; N,S: Nitrogen, sulfur-doped; QDs: Quantum dot.

their own merits and application ranges. According to the actual experimental conditions, the ideal synthesis method should be selected based on the principles of simplicity, economy, controllability, and large-scale production.

3. Water environment remediation

Currently, the emerging organic pollutants (e.g., antibiotics, endocrine disruptors, and personal care products) pose a serious threat to water quality safety.[41,42] Common treatment techniques, such as coagulation, sedimentation, filtration, and biological sludge, cannot effectively remove these organic pollutants because of their low biodegradability and chemical stability.[43] In addition to refractory organic pollutants, heavy metals, and microbial pollution, these threats also pose a threat to water quality security.[44,45] Photocatalysis is considered an important technology for remediation of water pollution, and the development of novel photocatalysts has become a focus of attention.[46-49] This section systematically introduces several typical applications of QD-modifying photocatalysts in water environmental remediation.

3.1. Photodegradation of organic pollutants

The efficiency of photocatalytic degradation of organic pollutants in water is mainly influenced by the ability to utilize light and the band structure of the photocatalyst.[7,46-49] The introduction of QDs can improve the light absorption, electron transfer, and electron–hole separation ability of photocatalysts. The photogenerated electrons and holes in the composite photocatalyst can react with O_2 and OH^- dissolved in water to form $O_2^{\bullet-}$, $^{\bullet}OH$, and $^1O_2$, thus effectively decomposing organic pollutants (**Equations 1–5**).[7] Moreover, some typical applications of QD-modifying photocatalysts for removing pollutants from water are summarized in Table 2.

$$QDs / photocatalysts + hv \rightarrow QDs / photocatalysts(h_{VB}^{+} + e_{CB}^{-}) \quad (1)$$

$$H_2O + h^+ \rightarrow {}^{\bullet}OH + H^+ \quad (2)$$

$$O_2 + e^- \rightarrow O_2^{\bullet-} \quad (3)$$

$$O_2^{\bullet-} + h^+ \rightarrow {}^1O_2 \quad (4)$$

$$h^+ / {}^{\bullet}OH / O_2^{\bullet-} / {}^1O_2 + organics \rightarrow small\ molecules \rightarrow CO_2 + H_2O \quad (5)$$

Seng *et al.*[50] successfully synthesized nitrogen-doped carbon (NC)QDs/g-C_3N_4 composites by doping NCQDs on the interlayer and surface of g-C_3N_4. When the content of NCQDs was 1.0 wt%, the degradation rate of methylene blue by NCQDs/g-C_3N_4 was 3.85 times higher than that of the pristine g-C_3N_4. In this system, $O_2^{\bullet-}$, $^{\bullet}OH$, and photogenerated holes all played crucial roles in the degradation of organic pollutants (Figure 3A).[50] Gao *et al.*[51] prepared composite photocatalysts g-C_3N_4/bismuth oxybromide (BiOBr)/MQDs doped with MQDs. g-C_3N_4/BiOBr/MQDs degraded 99% of 20 mg L^{-1} tetracycline

hydrochloride within 30 min, a rate that was 12 times higher than that achieved by pristine g-C_3N_4 (Figure 3B). MQDs can induce more vacancies to convert into $^1O_2$, which directly participates in the degradation of organic pollutants. Chen *et al.*[28] prepared porous hollow spheres of bismuth tungstate (Bi_2WO_6) doped with BPQDs. The BPQDs could form an energy bandgap that closely matches that of Bi_2WO_6, resulting in an S-type heterojunction for effective photogenerated charge separation (Figure 3C).

Heavy metal ions in industrial wastewater usually coexist with organic pollutants. The oxidative degradation of organic pollutants and the reductive removal of heavy metals can be synchronized via photocatalysis. Zhu *et al.*[36] prepared CQDs/$Bi_7O_9I_3$/g-C_3N_4 composite catalysts for the synchronous photocatalytic removal of chromium (Cr(VI)) and levofloxacin. The 0.5-CQD/$Bi_7O_9I_3$/g-C_3N_4 composite achieved a 100% reduction of Cr(VI) and 94.8% degradation of levofloxacin within 60 min. The reaction rate was 4.8 and 2.2 times higher than that of $Bi_7O_9I_3$/g-C_3N_4, respectively. Holes, $O_2^{\bullet-}$, and ·OH played a crucial role in the degradation of levofloxacin, and photogenerated electrons were the only dominant factor in Cr(VI) reduction (Figure 3D). Similarly, the synthesized bismuth(III) oxide (Bi_2O_3) QDs/C_3N_4 nanosheet photocatalysts could also simultaneously degrade TC and remove Cr(VI).[52] The removal rates of TC and Cr(VI) by Bi_2O_3 QDs/g-C_3N_4 were 2.0 and 7.1 times higher than those of pure g-C_3N_4 nanosheets, respectively.

3.2. Photocatalytic activation of peroxymonosulfate

The PMS (HSO_5^-) is widely used in the degradation and mineralization of refractory organic pollutants. PMS can be activated to produce $SO_4^{\bullet-}$ with strong redox potential and a wide pH range.[15] Photocatalytic activation has been recognized as a low-carbon PMS activation method with strong application prospects due to its high efficiency and environmental friendliness.[16] Doping electron-rich QDs can improve the conductivity and electron transfer behavior of photocatalysts, which is beneficial for activating PMS to produce ROS (**Equations 6–10**).[15-17]

$$e^- + HSO_5^- \rightarrow SO_4^{\bullet-} + OH^- \tag{6}$$

$$h^+ + HSO_5^- \rightarrow SO_5^{\bullet-} + H^+ \tag{7}$$

$$2SO_5^{\bullet-} \rightarrow 2SO_4^{\bullet-} + O_2 \tag{8}$$

$$SO_4^{\bullet-} + H_2O \rightarrow SO_4^- + {}^{\bullet}OH + H^+ \tag{9}$$

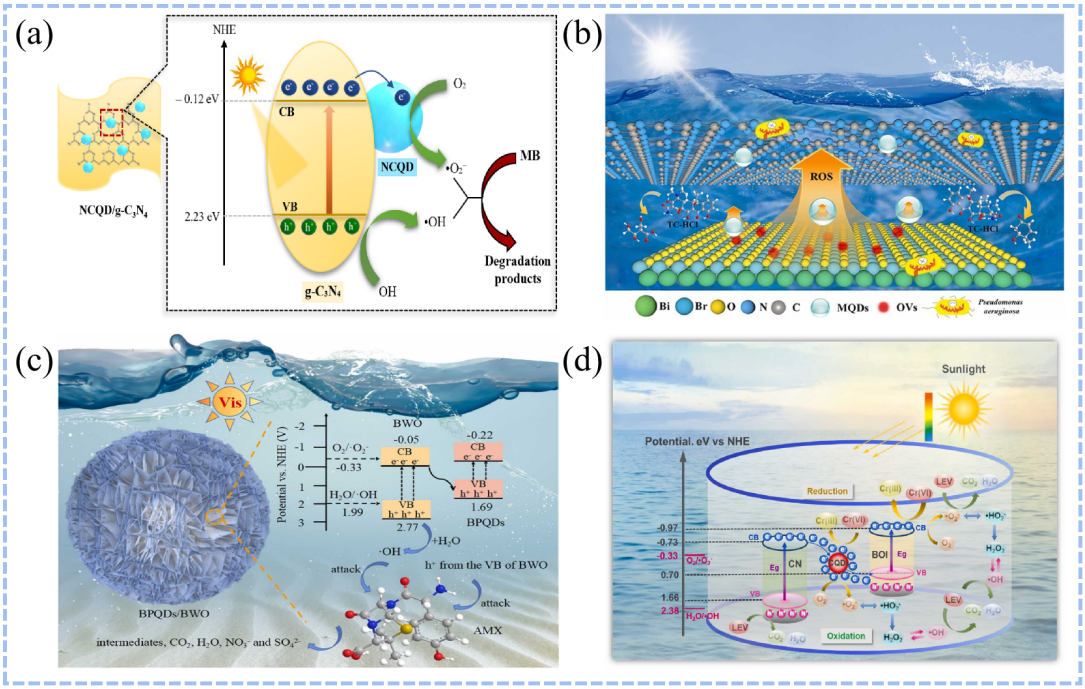

Figure 3. Schematic diagram of the QDs' catalytic reaction mechanism. (A) The mechanism for the degradation of methylene blue. Reprinted with permission from Seng *et al.*[50] Copyright © 2020 Elsevier. (B) Photocatalytic mechanism of gC3N4/bismuth oxybromide/MXene for the degradation of tetracycline hydrochloride. Reprinted with permission from Gao *et al.*[51] Copyright © 2023 Elsevier. (C) Photocatalytic mechanism of BPQDs/BWO for the degradation of amoxicillin. Reprinted with permission from Chen *et al.*[28] Copyright © 2023 Elsevier. (D) The mechanism for the reduction of chromium (VI) and degradation of levofloxacin. Reprinted with permission from Zhu *et al.*[36] Copyright © 2023 Elsevier.

$$4SO_4^{\bullet-} + 2H_2O \rightarrow 4HSO_4^- + {}^1O_2 \quad (10)$$

Ming *et al.*[17] synthesized CQD-doped functionalized CN to activate PMS for the degradation of BPA. Doping CQDs enhanced the catalyst's light absorption and charge separation, thereby facilitating PMS activation. Yang *et al.*[15] found that doping CDs into photocatalysts might play a dual role (Figure 4A). CDs enriched with carboxyl or pyrrole N tended to attract photogenerated electrons from CN, thus facilitating the separation of photocarriers. On the contrary, CDs rich in electron-donating graphitic N tended to form electron-rich regions at the CN main interface, thereby hindering the separation of charge carriers. Deng *et al.*[16] studied the enhancement effect of bismuth (Bi)/silver (Ag) double QD-doped photocatalyst (Bi-Ag@Bi_2MoO_6) on PMS activation (Figure 4B). The kinetic constants for the degradation of ciprofloxacin (CIP) by the Bi-Ag@Bi_2MoO_6/PMS system were 10 and 12 times higher than those for the Bi@Bi_2MoO_6/PMS and Bi_2MoO_6/PMS systems, respectively. CIP underwent a ring-opening reaction under the oxidation of $SO_4^{\bullet-}$, $^{\bullet}OH$, $^{\bullet}O_2^-$, and $^1O_2$. It was eventually degraded into carbon dioxide and water. This was because the formation of Bi/Ag double QDs remarkably improved the light-absorption performance of Bi_2MoO_6. Moreover, the synergistic doping of double QDs reduced the catalyst band gap from 2.72 to 2.12 eV.

Disinfection is crucial for ensuring water quality safety. Photocatalytic-based PMS technology not only remediates organic contamination but also inactivates pathogens in the wastewater. Jiang *et al.*[53] developed a PMS disinfection technology based on $^1O_2$ under visible light, using copper sulfide (CuS) QD-modified MIL-101 (Fe) (CSQDs@MF) (Figure 4C). This system could inactivate 7.5 *Escherichia coli* colonies within 60 min and could be applied across a wide pH range. The $^1O_2$ quantum yield of the CSQDs@MF system was increased by 80% compared with that of the MIL-101 (Fe) system. The enhancement of electron and energy transfer in this system was the reason for the increase in the production rate of $^1O_2$. The doping of CuS QDs enhanced photocatalytic activity by increasing visible light absorption, accelerating electron transfer, and improving charge–carrier separation.

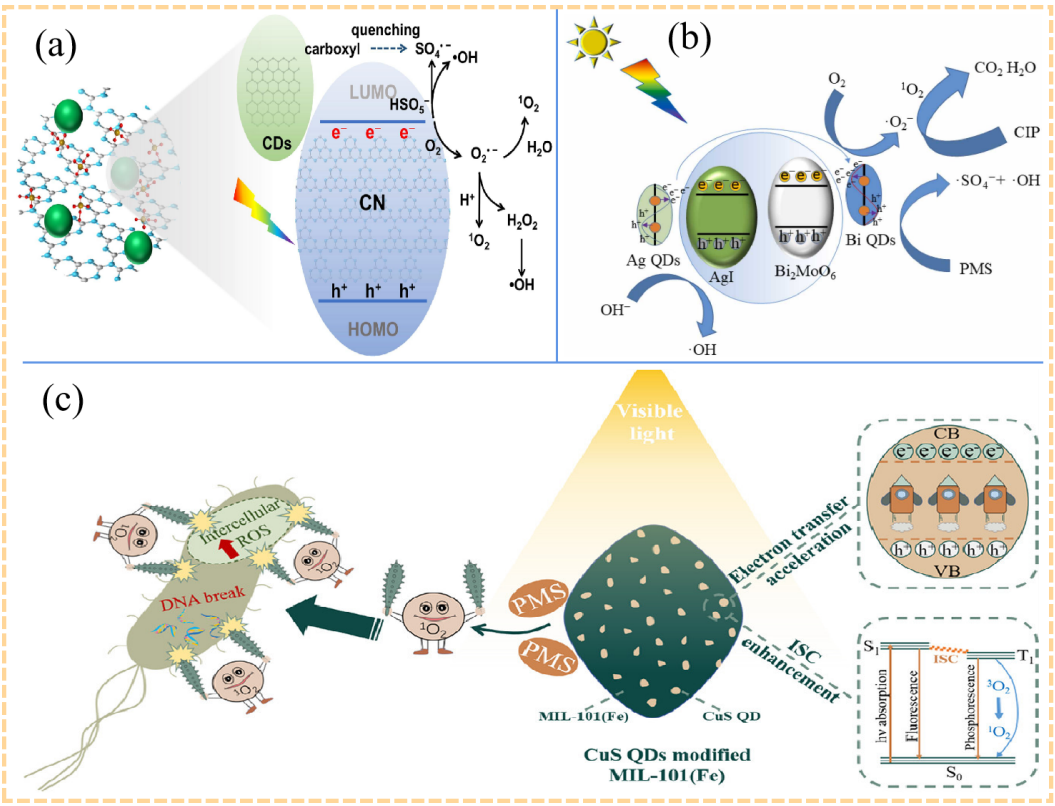

Figure 4. Schematic diagram of the mechanism of QDs activating PMS. (A) Photocatalytic mechanism of PMS activation by ^{1}N-CDs/CN and ca-CDs/CN. Reprinted with permission from Yang *et al.*[15] Copyright © 2023 Elsevier. (B) The mechanism of PMS activation by Bi-Ag@Bi_2MoO_6. Reprinted with permission from Deng *et al.*[16] Copyright © 2023 Elsevier. (C) The mechanism of PMS activation by CSQDs@MF for inactivating *Escherichia coli*. Reprinted with permission from Jiang *et al.*[53] Copyright © 2023 Elsevier.
Abbreviations: CD: Carbon dot; CN: Carbon nitride; PMS: Peroxymonosulfate; QD: Quantum dot.

The summary highlights that the most common types of QDs used to modify photocatalysts are CQDs, BNQDs, $Ti_3C_2T_x$ QDs, BPQDs, and MCQDs. The doping of QDs substantially enhances photocatalytic performance, effectively activates PMS, and increases the kinetic rate of pollutant removal by several times to a dozen times (Table 2).[54,55] The doping of QDs not only optimizes the morphology and structure of photocatalysts but also enhances their performance by increasing surface area, improving charge-carrier separation efficiency, accelerating electron transfer, and narrowing the band gap.[56,57]

3.3. Production and application of hydrogen peroxide

Hydrogen peroxide, a versatile and environmentally friendly oxidant, is widely used for water purification and disinfection.[58] Moreover, the product of H_2O_2 after use is only water, which does not produce by-products with secondary pollution.[59] The anthraquinone method is currently the mainstream for the industrial production of H_2O_2. However, it has some limitations, such as high cost, complex process, and the production of toxic by-products.[59] Recently, researchers have shown great interest in using photocatalytic methods to produce H_2O_2. In the presence of light, a photocatalyst can produce free electrons to promote the reduction of O_2 to generate H_2O_2 (**Equations 3 and 11**).[59,60] However, the efficiency of traditional photocatalysts such as TiO_2 and g-C_3N_4 in producing H_2O_2 is low, mainly due to their poor charge separation efficiency and weak light absorption.[61] The doping of QDs can expand the light absorption wavelength, promote electron–hole separation, and accelerate electron transfer, thereby overcoming the shortcomings of traditional photocatalysts. This section introduces the photocatalytic production of H_2O_2 and its application in pollutant degradation. Some representative reports are summarized in Table 3.

$$O_2^{\bullet-} + 2H^+ + e^- \rightarrow H_2O_2 \tag{11}$$

Zheng *et al.*[61] synthesized SNGQD/TiO_2 for H_2O_2 production by modifying TiO_2 with S- and N-co-doped graphene QDs (SNGQDs). SNGQDs were uniformly dispersed on the surface of TiO_2, thereby extending the light absorption and enhancing electron migration. Under light irradiation, the H_2O_2 yield of SNGQD/TiO_2 (451 μmol L^{-1}) was 3.2 times higher than that of pristine TiO_2 and considerably higher than those of the GQD/TiO_2 and nitrogen-doped-GQD/TiO_2 systems. The free energy diagrams for each step of the oxygen reduction reaction on SNGQDs are shown in Figure 5A. Two O_2 molecules were first adsorbed on the SNGQDs. The adsorbed two O_2 were rapidly converted to two *OOH by coupling protons and electrons. Then two *OOH combined with two protons and electrons to form two H_2O_2 molecules. The free energy decreased during each step of H_2O_2 production in the system, indicating that the process was thermodynamically spontaneous. The increase in H_2O_2 production in the SNGQD/TiO_2 system was attributed to the enhanced two-electron reduction of oxygen (Figure 5B). Ma *et al.*[33] anchored CNQDs onto g-C_3N_4 nanosheets to form a homogeneous structure (HJ-C_3N_4), greatly improving performance without doping metal elements. Under visible light, the H_2O_2 yield of HJ-C_3N_4 in water reached 115 μmol L^{-1}, which was 8.6 times higher than that of g-C_3N_4 nanosheets. The excellent photocatalytic efficiency was attributed to the band alignment of the homogeneous junction structure, which facilitated efficient electron–hole separation, whereas CNQDs inhibited electron–hole recombination. In addition, doping CNQDs broadened the light-absorption wavelength range of g-C_3N_4 nanosheets.

The photo-Fenton method can accelerate the regeneration of Fe^{2+} and the decomposition of H_2O_2, producing ROS that oxidize target organic pollutants. This compensates for the shortcomings of the conventional Fenton method (**Equations 12–14**).[62-64] Shi *et al.*[60] synthesized a self-sufficient photo-Fenton system for the degradation of oxytetracycline (OTC) by coupling ultrathin porous g-C_3N_4 nanosheets with amorphous iron(III) oxyhydroxide (FeOOH) QDs (Figure 5C). The *in situ*-generated H_2O_2 from g-C_3N_4, together with FeOOH QDs, formed the photo-Fenton system, which could enhance the degradation of OTC. After the Fe^{3+} was reduced to Fe^{2+} by the transferred photogenerated electrons, Fe^{2+} reacted with H_2O_2 to generate $^\bullet$OH to degrade OTC. Then, Fe^{3+} was recycled by obtaining electrons to be reduced to Fe^{2+} under light (**Equations 15–17**) (Figure 5D).[63] Therefore, the synergistic effect of FeOOH QDs and g-C_3N_4 nanosheets with *in situ* generated H_2O_2 could effectively improve the performance of photocatalytic degradation of OTC.

$$e^- + H_2O_2 \rightarrow 2^\bullet OH \tag{12}$$

$$^\bullet OH + O_2^{\bullet-} \rightarrow {}^1O_2 + OH^- \tag{13}$$

$$h^+ + H_2O \rightarrow {}^\bullet OH + H^+ \tag{14}$$

$$Fe^{3+} + e^- \rightarrow Fe^{2+} \tag{15}$$

$$Fe^{2+} + H_2O_2 \rightarrow Fe^{3+} + {}^\bullet OH + OH^- \tag{16}$$

$$Fe^{3+} + H_2O + hv \rightarrow Fe^{2+} + {}^\bullet OH + H^+ \tag{17}$$

The photocatalytic method provides an efficient and environmentally friendly approach to H_2O_2 production. Moreover, the self-generated H_2O_2 in the *in situ*

Table 2. Summary of the reported representative QD-modifying photocatalysts for the removal of pollutants

Composite photocatalyst	Type of QDs	Role of QDs	Experimental condition	Pollutants	Main active species	Removal performance	Ref.
Bi-Ag@ Bi_2MoO_6-400	Bi/Ag double QD	Enhances visible light absorption and narrow-bandgap	300 W Xe lamp; 60 min; PMS: 0.075 mM	50 mL 10 mg L^{-1} ciprofloxacin	$O_2^{\bullet-}$, $SO_4^{\bullet-}$, $^{\bullet}OH$, and $^1O_2$	Bi-Ag@Bi_2MoO_6-400 (100%), Bi_2MoO_6-400 (38.05%), Bi@Bi_2MoO_6-400 (52.58%), Ag@Bi_2MoO_6-400 (73.83%)	16
CQDs/ PCNC-2	CQDs	Increase surface area, promote e^-/H^+ separation, enhance visible light absorption, and narrow band gap	300 W Xe lamp (350 mW cm^{-2}); 60 min; PMS: 0.097 mM	20 mg L^{-1} BPA	$O_2^{\bullet-}$, H^+ $SO_4^{\bullet-}$, and $^{\bullet}OH$	CQDs/PCNC-2 (95.0%), PCN (24.0%)	17
2BPQDs/BWO	BPQDs	Promote e^-/H^+ separation	300 W Xe lamp; 60 min; solvent: water	20 mg L^{-1} amoxicillin	H^+ and $^{\bullet}OH$	2BPQDs/BWO (94.5%)	28
1BQPN	BNQDs	Promote e^-/H^+ separation and carrier migration	blue LED lamp; 32.6 mW cm^{-2}); 20 min; solvent: water	10 mg L^{-1} naproxen	$O_2^{\bullet-}$ and H^+	1BQPN (0.1176 min^{-1}); CN (0.0151 min^{-1})	34
0.5 wt% CQD/ BOI/CN	CQD	Promote e^-/H^+ separation and enhance visible light absorption	300 W Xe lamp (100 mW cm^{-2}); 60 min	20 mg L^{-1} Cr(VI) 20; 20 mg L^{-1} levofloxacin	$O_2^{\bullet-}$, H^+, and $^{\bullet}OH$	0.5-CQD/BOI/CN (100% Cr(VI); 94.8% levofloxacin)	36
g-C_3N_4/BiOBr/ MQDs	$Ti_3C_2T_x$ QDs	Suppress electron return, accelerate photo-carrier transport	300 W Xe lamp; 30 min; solvent: water	20 mg L^{-1} TCH	$O_2^{\bullet-}$, H^+, $^{\bullet}OH$, and $^1O_2$	g-C_3N_4/BiOBr/MQDs (99%); g-C_3N_4 (approximately 50%)	51
0.7 wt% Bi_2O_3 QDs/g-C_3N_4	Bi_2O_3 QDs	Promote e^-/H^+ separation	350 W Xe lamp; TC: 120 min Cr(VI): 60 min; solvent: water	10 mg L^{-1} tetracycline; 10 mg L^{-1} Cr(VI)	$O_2^{\bullet-}$, H^+, and $^{\bullet}OH$	0.7wt%Bi_2O_3 QDs/g-C_3N_4 (87.9% Cr(VI); 82.5% tetracycline), g-C_3N_4 (12.4% Cr(VI); 41.3% tetracycline)	52
1 wt% NCQDs/g-C_3N_4	NCQDs	Improve converted photoluminescence property, promote e^-/H^+ separation, narrow bandgap	350 W Xe lamp; 90 min; solvent: water	4 mg L^{-1} indomethacin	$O_2^{\bullet-}$ and H^+	NCQDs/g-C_3N_4 (91.5%), g-C_3N_4 (16.0%)	54
3 wt% CQDs/ Ag_2CO_3, 3N-CQDs/ Ag_2CO_3	CQDs, NCQDs	increase surface area, decrease charge transfer resistance, promote e^-/H^+ separation	350 W Xe lamp; 150 min; solvent: water	20 mg L^{-1} phenol	$O_2^{\bullet-}$, H^+, and $^{\bullet}OH$	N-CQDs/Ag_2CO_3 (54.60%), CQDs/Ag_2CO_3 (20.66%)	55
1% CQDs/ Sb_2WO_6	CQDs	Promote e^-/H^+ separation, convert long wavelength light from 550–850 nm to short wavelength light from 440–500 nm	Xe lamp; 30 min; solvent: water	10 mg L^{-1} rhodamine B	$O_2^{\bullet-}$ and H^+	1%CQDs/Sb_2WO_6 (83%), Sb_2WO_6 (8%) 1%CQDs/Sb_2WO_6; The kinetic constant of 1%CQDs/Sb_2WO_6 is nearly 7 times higher than that of Sb_2WO_6	56
3 wt% CQDs/ Bi_2WO_6	CQDs	Promote e^-/H^+ separation and enhance visible light absorption	300 W Xe lamp; 40 min; solvent: water	20 mg L^{-1} tetracycline	$O_2^{\bullet-}$, H^+, and $^{\bullet}OH$	3wt%CQDs/Bi_2WO_6 (89.0%)	57

Abbreviations: Ag: Silver; Bi: Bismuth; Bi_2O_3: Bismuth(III) oxide; Bi_2WO_6: Bismuth tungstate; BiOBr: Bismuth oxybromide; BN: Boron nitride; BP: Black phosphorus; BQPN: Boron nitride quantum dots modified P-doped g-C_3N_4 photocatalyst; C: Carbon; CN: Carbon nitride; M: Mxene; NC: Nitrogen-doped carbon; PCN: Polymer carbon nitride; PCNC: Carbon quantum dots functionalized polymer carbon nitride; PMS: Peroxymonosulfate; QD: Quantum dot; TCH: Tetracycline hydrochloride; Xe: Xenon.

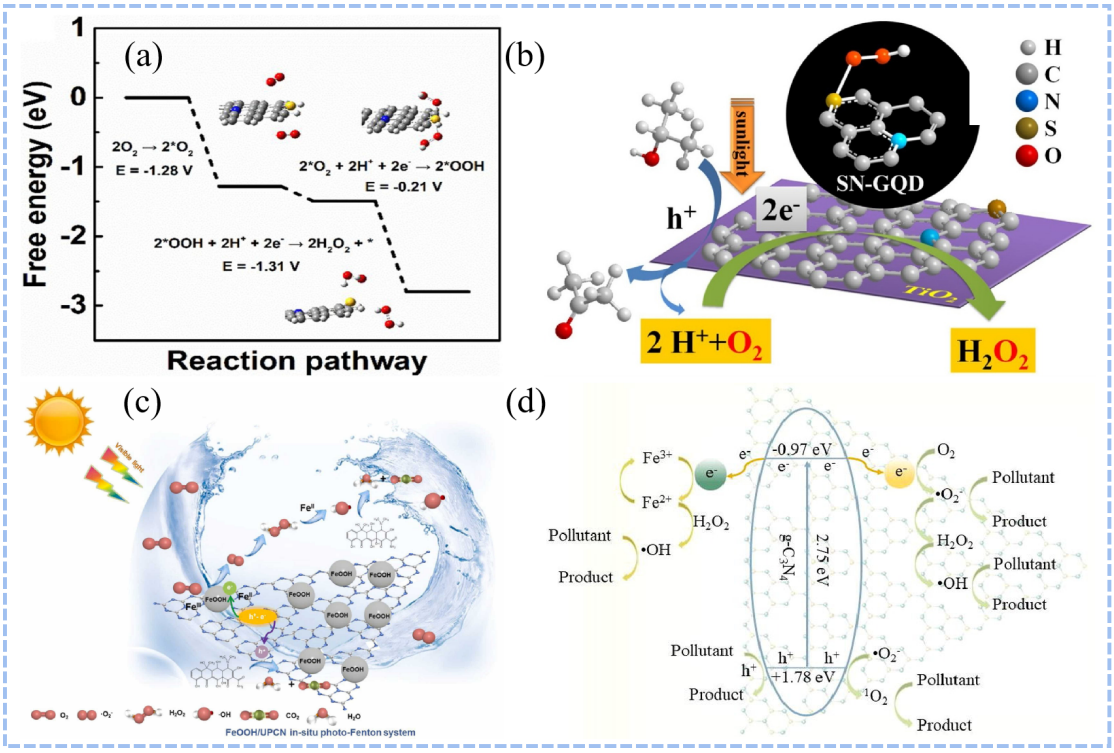

Figure 5. Schematic diagram of QD's catalytic production of H_2O_2. (A) Free energy of oxygen reduction reaction pathways. (B) Photocatalytic mechanism of SNGQDs for H_2O_2 production. Reprinted with permission from Zheng *et al.*[61] Copyright © 2018 Elsevier. (C) Photo-Fenton mechanism of the FeOOH/UPCN composite system. Reprinted with permission from Shi *et al.*[60] Copyright © 2022 Elsevier. (D) The mechanism for the degradation of oxytetracycline. Reprinted with permission from Zhang *et al.*[63] Copyright © 2020 Elsevier.
Abbreviations: FeOOH: Iron(III) oxyhydroxide; QD: Quantum dot; SNGQDs: S- and N-co-doped graphene quantum dots; UPCN: Ultrathin porous g-C_3N_4.

photo-Fenton system can eliminate the need for H_2O_2 transportation and addition processes. Furthermore, the doping of QDs generally improves H_2O_2 production and organic pollutant degradation by promoting electron–hole separation, enhancing visible light absorption, accelerating electron transfer, heightening O_2 activation, and facilitating the reduction of Fe^{3+} to Fe^{2+} (Table 3).

4. Challenges and prospects

The following suggestions and future perspectives are proposed to address the current challenges associated with the preparation and application of QD-modified photocatalysts:

(i) The selection of QD synthesis methods is closely related to the type of QDs. At present, although the synthesis of QDs has made great progress, some types of QDs, such as BPQDs, MQDs, and BNQDs, still require more complex processes and the use of specialized reagents. In the future, lower-cost and more environmentally friendly synthetic technologies should be explored.

(ii) At present, the synthesis and application of QDs are mostly limited to the laboratory, and there are few application studies in the actual environment. The development of large-scale continuous synthesis processes for QDs deserves future attention.

(iii) Artificial intelligence (AI) is profoundly transforming the research, development, and production paradigm of QDs. Through data-driven strategies and algorithm optimization, AI has greatly improved the research and development efficiency, material performance, and industrialization process of QDs. AI can accelerate the synthesis and optimization of materials and reduce research and development costs; it can accurately predict and regulate material properties to realize "on-demand design".

(iv) The application of QD-modifying photocatalysts is often limited to their oxidation or reduction effects. We should vigorously develop the simultaneous use of oxidation and reduction potentials of catalysts and promote the use of photocatalysts and solar energy.

(v) Photocatalysts require long-term use to reduce the cost of actual environmental purification. The powder

Table 3. Summary of the reported representative QD-modifying photocatalysts for the evolution of H_2O_2

Composite photocatalyst	Type of QDs	Role of QDs	Experimental condition	Pollutants	Main active species	Performance	Ref.
CNQDs/g-C_3N_4	CNQDs	Promote e^-/H^+ separation, enhances visible light absorption	300 W Xe lamp (109 mW cm^{-2}); 60 min; solvent: 20 mL water	–	–	CNQDs/g-C_3N_4 (115 μmol L^{-1} H_2O_2), g-C_3N_4 (14 μmol L^{-1} H_2O_2)	33
20% FeOOH QDs/UPCN	FeOOH QDs	Promote e^-/H^+ separation, enhance visible light absorption, and Fe^{3+} in FeOOH QDs is reduced to Fe^{2+} by photoexcited electrons	300 W Xe lamp; 120 min; solvent: 50 mL water	20 mg L^{-1} OTC	$O_2^{\bullet-}$, H^+, and $^{\bullet}OH$	20%FeOOH/UPCN (86.23% OTC), UPCN (30.00% OTC; 23.91 μmol L^{-1} H_2O_2). H_2O_2 is not detected in the FeOOH/UPCN system because the generated H_2O_2 is consumed by Fe^{2+} to form Fe^{3+} and $^{\bullet}OH$.	60
SNGQDs/TiO_2	SNGQDs	Improve conversion property, promote e^-/H^+ separation, narrow band gap, and accelerate two-electron reduction	550 W Xe lamp; 60 min; solvent: 47 mL water + 3 mL 2-propanol	–	–	SNGQDs/TiO_2 (451 μmol L^{-1} H_2O_2), TiO_2 (140 μmol L^{-1} H_2O_2)	61
FeOOH QDs/CQDs/g-C_3N_4	FeOOH QDs, CQDs	Accelerate electron transfer, enhance activation of O_2, promote e^-/H^+ separation, Fe^{3+} in FeOOH QDs is reduced to Fe^{2+} by photoexcited electrons	300 W Xe lamp (λ ≥ 420 nm); 60 min; solvent: 10 mL of isopropanol + 90 mL water	100 mL 10 mg L^{-1} OTC	$O_2^{\bullet-}$, H^+, $^{\bullet}OH$, and $^1O_2$	FeOOH QDs/CQDs/g-C_3N_4 (85.5% OTC; 224.24 μmol g^{-1} H_2O_2), g-C_3N_4 (46.2% OTC)	63
HTNT-CQDs	CQDs	Accelerates the reduction of O_2 to H_2O_2 and prevents the decomposition of H_2O_2	350 W Xe lamp (λ > 365 nm); 60 min; 15 mL solvent: water	–	–	HTNT-CQDs (84.8 μmol L^{-1} H_2O_2), HTNT (H_2O_2 is not detected)	64

Abbreviations: C: Carbon; CN: Carbon nitride; FeOOH: Iron(III) oxyhydroxide; H_2O_2: Hydrogen peroxide; HTNT: Proton-form titania nanotube; NC: Nitrogen-doped carbon; OTC: Oxytetracycline; QD: Quantum dot; UPCN: Ultrathin porous g-C_3N_4; Xe: Xenon.

QD-modifying photocatalysts are not favorable for reuse in practical applications. Developing a continuous-flow photocatalytic reactor can effectively separate catalysts and pollutants, and promote the utilization rate of photocatalysts.

(vi) The ongoing studies on water pollution remediation focus on simulated wastewater in the laboratory. The actual wastewater has a complex composition and a wide range of pollutants. In the future, studies on multiple pollutants in wastewater should be increased, and actual water quality conditions (such as pH, temperature, and contaminant concentrations) should be considered. Critically, contaminants may be converted to more toxic intermediates during photocatalysis. Thus, the ecological safety of the treated wastewater should also be verified.

(vii) The reported studies mainly focus on the enhancement of photocatalyst performance with QDs, although there is an insufficient study on the mechanism of the QD-modifying photocatalysts application process. In future studies, the latest theoretical calculations and advanced characterization techniques should be combined to elucidate the complex mechanisms of photocatalytic reactions.

(viii) Quantum dots can induce various types of genetic material damage, which subsequently triggers a series of adverse cellular consequences, including apoptosis, cell cycle arrest, and senescence. QDs can damage DNA via their intrinsic nanostructures or released metal ions. As is well known, the physicochemical

properties of nanomaterials determine their toxicity. Accordingly, QDs closer to practical application should be the focus of future research, which can provide greater guidance for their safe application.

5. Conclusion

Photocatalytic technology offers high efficiency and energy savings, and thus plays an increasingly essential role in water remediation and in alleviating the energy crisis. However, traditional photocatalysts still face challenges, such as narrow light absorption ranges and facile electron–hole recombination. QDs are often doped into photocatalysts to enhance their photocatalytic performance, as QDs possess excellent photoelectric properties. This review systematically summarizes the current synthesis methods of QDs (CQDs, GQDs, MQDs, BPQDs, and MCQDs). Moreover, the study progress of various QD-modifying photocatalysts in pollutant removal and H_2O_2 generation is introduced in detail.

Acknowledgments

None.

Funding

The work was supported by the Project of Key Scientific and Technological Research in Key Areas of the Corps (2023AB034) and Open Research Project of the Key Laboratory of Northwest Oasis Water-Saving Agriculture (2023OWSL-01).

Conflict of interest

The authors declare they have no competing interests.

Author contributions

Conceptualization: Shuan Liu, Yuhui Yang
Writing–original draft: Shuan Liu, Yinghao Xue, Qixin Pan
Writing–review & editing: Xingpeng Wang, Weixuan Huang, Yunqian Song

Availability of data

Not applicable.

References

1. Yan ZQ, Yin WQ, Xu MC, *et al*. Photocatalysis for synergistic water remediation and H2 production: a review. *Chem Eng J*. 2023;472:145066.

   doi: 10.1016/j.cej.2023.145066

2. Ran MX, Hu YK, Cao JZ, *et al*. Piezo-photocatalytic-Fenton-like ternary coupling system for enhanced resourceful conversion of organic pollutant. *Water Res*. 2025;285:124122.

   doi: 10.1016/j.watres.2025.124122

3. Cao JZ, Zhang WW, Lv WJ, *et al*. Electron transfer-mediated enhanced sustained degradation of refractory high ionization potential organic pollutants via a self-floating photo-Fenton membrane. *Sci Bull*. 2026;71(3):577-586.

   doi: 10.1016/j.scib.2025.12.052

4. Fu JC, Xiao SZ, Cao JZ, *et al*. Mass transfer-enhanced photothermal membranes with synergistic light utilization for high-turbidity wastewater purification. *Angew Chem Int Ed*. 2025;64(11):e202421800.

   doi: 10.1002/anie.202421800

5. Liang LH, Cao JZ, Chen Z, *et al*. Harnessing Fe–Mo atomic interfaces for boosted electron transfer and ROS generation in sustainable pollutant degradation. *Environ Sci Technol*. 2025;59(42):22914-22926.

   doi: 10.1021/acs.est.5c06307

6. Chang SK, Abbasi QA, Abbasi Z, *et al*. Rapid pH-dependent photocatalytic degradation of methylene blue by CdS nanorods synthesized through hydrothermal process. *Arab J Chem*. 2023;17(1):105422.

   doi: 10.1016/j.arabjc.2023.105422

7. Sun P, Xing ZP, Li ZZ, Zhou W. Recent advances in quantum dots photocatalysts. *Chem Eng J*. 2023;458:141399.

   doi: 10.1016/j.cej.2023.141399

8. Nozik AJ, Beard MC, Luther JM. Semiconductor quantum dots and quantum dot arrays and applications of multiple exciton generation to third-generation photovoltaic solar cells. *Chem Rev*. 2010;110(11):6873-6890.

   doi: 10.1021/cr900289f

9. Ai L, Yang YS, Wang BY, *et al*. Insights into photoluminescence mechanisms of carbon dots: advances and perspectives. *Sci Bull*. 2021;66(8):839-856.

   doi: 10.1016/j.scib.2020.12.015

10. Lu ZY, Li CM, Han J, *et al*. Construction 0D/2D heterojunction by highly dispersed Ni2P QDs loaded on the ultrathin g-C3N4 surface towards superhigh photocatalytic and photoelectric performance. *Appl Catal B Environ*. 2018;237:919-926.

    doi: 10.1016/j.apcatb.2018.06.062

11. Moon H, Lee C, Lee W. Stability of quantum dots, quantum dot films, and quantum dot light-emitting diodes for display applications. *Adv Mater*. 2019;31(34):1804294.

    doi: 10.1002/adma.201804294

12. Peng X. Band gap and composition engineering on a nanocrystal (BCEN) in solution. *Acc Chem Res*. 2010;43(11):1387-1395.

    doi: 10.1021/ar100025m

13. Gao YJ, Li XB, Wu HL. Exceptional catalytic nature of

quantum dots for photocatalytic hydrogen evolution without external cocatalysts. *Adv Funct Mater*. 2018;28(33):1801769.

doi: 10.1002/adfm.201801769

14. Raziq F, Hayat A, Humayun M. Photocatalytic solar fuel production and environmental remediation through experimental and DFT based research on CdSe-QDs-coupled P-doped-g-C3N4 composites. *Appl Catal B Environ*. 2020;270:118867.

doi: 10.1016/j.apcatb.2020.118867

15. Yang P, Shen A, Zhu ZQ, *et al*. Construction of carbon nitride-based heterojunction as photocatalyst for peroxymonosulfate activation: important role of carbon dots in enhancing photocatalytic activity. *Chem Eng J*. 2023;464:142724.

doi: 10.1016/j.cej.2023.142724

16. Deng Y, Wang JT, Wang J, *et al*. In situ growth of Bi/Ag double quantum dots on hollow Bi2MoO6 microspheres: enhancement of the surface plasmon resonance effect on PMS activation. *Appl Catal B Environ*. 2023;338:123041.

doi: 10.1016/j.apcatb.2023.123041

17. Ming HB, Wei DL, Yang Y, *et al*. Photocatalytic activation of peroxymonosulfate by carbon quantum dots functionalized carbon nitride for efficient degradation of bisphenol A under visible-light irradiation. *Chem Eng J*. 2021;424:130296.

doi: 10.1016/j.cej.2021.130296

18. Sharma S, Dutta V, Singh P, *et al*. Carbon quantum dot supported semiconductor photocatalysts for efficient degradation of organic pollutants in water: a review. *J Clean Prod*. 2019;228:755-769.

doi: 10.1016/j.jclepro.2019.04.292

19. Cheng CY, Liang QH, Yan M, *et al*. Advances in preparation, mechanism and applications of graphene quantum dots/semiconductor composite photocatalysts: a review. *J Hazard Mater*. 2022;424:127721.

doi: 10.1016/j.jhazmat.2021.127721

20. Long CH, Jiang ZX, Shangguan JF, Qing TP, Zhang P, Feng B. Applications of carbon dots in environmental pollution control: a review. *Chem Eng J*. 2021;406:126848.

doi: 10.1016/j.cej.2020.126848

21. Rani UA, Ng LY, Ng CY, Mahmoudi E. A review of carbon quantum dots and their applications in wastewater treatment. *Adv Colloid Interface Sci*. 2020;278:102124.

doi: 10.1016/j.cis.2020.102124

22. Mei AX, Xu ZJ, Wang XY, *et al*. Photocatalytic materials modified with carbon quantum dots for the degradation of organic pollutants under visible light: a review. *Environ Res*. 2022;214:114160.

doi: 10.1016/j.envres.2022.114160

23. Deng H, Hui YX, Zhang C, *et al*. MXene-derived quantum dots based photocatalysts: synthesis, application, prospects, and challenges. *Chin Chem Lett*. 2024;35(6):109078.

doi: 10.1016/j.cclet.2023.109078

24. Peng J, Gao W, Gupta BK. Graphene quantum dots derived from carbon fibers. *Nano Lett*. 2012;12(2):844-849.

doi: 10.1021/nl2038979

25. Li YJ, Ding L, Guo YC, Liang ZQ, Cui HZ, Tian J. Boosting the photocatalytic ability of g-C3N4 for hydrogen production by Ti3C2 MXene quantum dots. *ACS Appl Mater Interfaces*. 2019;11(44):41440-41447.

doi: 10.1021/acsami.9b14985

26. Zhuo S, Shao M, Lee ST. Upconversion and downconversion fluorescent graphene quantum dots: ultrasonic preparation and photocatalysis. *ACS Nano*. 2012;6(2):1059-1064.

doi: 10.1021/nn2040395

27. Luo ZM, Qi GQ, Chen KY, *et al*. Microwave-assisted preparation of white fluorescent graphene quantum dots as a novel phosphor for enhanced white-light-emitting diodes. *Adv Funct Mater*. 2016;26(16):2739-2744.

doi: 10.1002/adfm.201505044

28. Chen LJ, Wang CG, Liu GZ, *et al*. Anchoring black phosphorous quantum dots on Bi2WO6 porous hollow spheres: a novel 0D/3D S-scheme photocatalyst for efficient degradation of amoxicillin under visible light. *J Hazard Mater*. 2023;443:130326.

doi: 10.1016/j.jhazmat.2022.130326

29. Zhang HJ, Wu WX, Li Y, *et al*. Enhanced photocatalytic degradation of ciprofloxacin using novel C-dot@nitrogen deficient g-C3N4: synergistic effect of nitrogen defects and C-dots. *Appl Surf Sci*. 2019;465:450-458.

doi: 10.1016/j.apsusc.2018.09.183

30. Zheng LY, Chi YW, Dong YQ, Lin JP, Wang BB. Electrochemiluminescence of water-soluble carbon nanocrystals released electrochemically from graphite. *J Am Chem Soc*. 2009;131(13):4564-4565.

doi: 10.1021/ja809073f

31. Zhang M, Bai LL, Shang WH, *et al*. Facile synthesis of water-soluble, highly fluorescent graphene quantum dots as a robust biological label for stem cells. *J Mater Chem*. 2012;22(15):7461-7467.

doi: 10.1039/C2JM16835A

32. Dong Y, Shao J, Chen C. Blue luminescent graphene quantum dots and graphene oxide prepared by tuning the carbonization degree of citric acid. *Carbon*. 2012;50(12):4738-4743.

doi: 10.1016/j.carbon.2012.06.002

33. Ma PJ, Zhang X, Wang C, *et al*. Band alignment of

homojunction by anchoring CN quantum dots on g-C3N4 (0D/2D) enhance photocatalytic hydrogen peroxide evolution. *Appl Catal B Environ*. 2022;300:120736.

doi: 10.1016/j.apcatb.2021.120736

34. Li DG, Liu Y, Wen CH, *et al*. Construction of dual transfer channels in graphitic carbon nitride photocatalyst for high-efficiency environmental pollution remediation: enhanced exciton dissociation and carrier migration. *J Hazard Mater*. 2022;436:129171.

doi: 10.1016/j.jhazmat.2022.129171

35. Qu YN, Xu XJ, Huang RL, Qi W, Su RX, He ZM. Enhanced photocatalytic degradation of antibiotics in water over functionalized N,S-doped carbon quantum dots embedded ZnO nanoflowers under sunlight irradiation. *Chem Eng J*. 2020;382:123016.

doi: 10.1016/j.cej.2019.123016

36. Zhu LL, Shen DK, Zhang HY, Luo KH, Li C. Fabrication of Z-scheme Bi7O9I3/g-C3N4 heterojunction modified by carbon quantum dots for synchronous photocatalytic removal of Cr(VI) and organic pollutants. *J Hazard Mater*. 2023;446:130663.

doi: 10.1016/j.jhazmat.2022.130663

37. Das R, Bandyopadhyay R, Pramanik P. Carbon quantum dots from natural resource: a review. *Mater Today Chem*. 2018;8:96-109.

doi: 10.1016/j.mtchem.2018.03.003

38. Medeiros TVD, Manioudakis J, Noun F. Microwave-assisted synthesis of carbon dots and their applications. *J Mater Chem C*. 2019;7(24):7175-7195.

doi: 10.1039/C9TC01640F

39. Ding YY, Gong XJ, Liu Y, *et al*. Facile preparation of bright orange fluorescent carbon dots and the constructed biosensing platform for the detection of pH in living cells. *Talanta*. 2018;189:8-15.

doi: 10.1016/j.talanta.2018.06.060

40. Tang L, Ji R, Cao X. Deep ultraviolet photoluminescence of water-soluble self-passivated graphene quantum dots. *ACS Nano*. 2012;6(6):5102-5110.

doi: 10.1021/nn300760g

41. Bexfield LM, Toccalino PL, Belitz K, Foreman WT, Furlong ET. Hormones and pharmaceuticals in groundwater used as a source of drinking water across the United States. *Environ Sci Technol*. 2019;53(6):2950-2960.

doi: 10.1021/acs.est.8b05592

42. Kim SC, Carlson K. Occurrence of ionophore antibiotics in water and sediments of a mixed-landscape watershed. *Water Res*. 2006;40(13):2549-2560.

doi: 10.1016/j.watres.2006.04.036

43. Wang HH, Duan YH, Fei GQ, Yan TJ, Kang YM, Dionysiou DD. Design, synthesis and modification of 2D nanomaterials-based photocatalysts for pollutant degradation and photodegradation experiments from lab-scale to grand-scale. *Chem Eng J*. 2023;477:147219.

doi: 10.1016/j.cej.2023.147219

44. Wang WH, Gao P, Yang C, *et al*. Separable and reactivated magnetic mZVAl/nFe3O4 composite induced by ball milling for efficient adsorption-reduction-sequestration of aqueous Cr(VI). *Sep Purif Technol*. 2022;288:120689.

doi: 10.1016/j.seppur.2022.120689

45. Li X, Shi J, Sun H, Lin Z. Hormetic dose-dependent response about typical antibiotics and their mixtures on plasmid conjugative transfer of Escherichia coli and its relationship with toxic effects on growth. *Ecotoxicol Environ Saf*. 2020;205:111300.

doi: 10.1016/j.ecoenv.2020.111300

46. Zhang XY, Yu WC, Guo YJ, *et al*. Recent advances in photoelectrocatalytic advanced oxidation processes: from mechanism understanding to catalyst design and actual applications. *Chem Eng J*. 2023;455:140801.

doi: 10.1016/j.cej.2022.140801

47. Li XF, Qiu YL, Zhu ZL, Zhang H, Yin DQ. Novel recyclable Z-scheme g-C3N4/carbon nanotubes/Bi25FeO40 heterostructure with enhanced visible-light photocatalytic performance towards tetracycline degradation. *Chem Eng J*. 2022;429:132130.

doi: 10.1016/j.cej.2021.132130

48. Wang R, Lu KQ, Tang ZR, Xu YJ. Recent progress in carbon quantum dots: synthesis, properties and applications in photocatalysis. *J Mater Chem A*. 2017;5(8):3717.

doi: 10.1039/c6ta08660h

49. Lim SY, Shen W, Gao ZQ. Carbon quantum dots and their applications. *Chem Soc Rev*. 2015;44(1):362.

doi: 10.1039/c4cs00269e

50. Seng RX, Tan LL, Lee W, Ong WJ, Chai SP. Nitrogen-doped carbon quantum dots-decorated 2D graphitic carbon nitride as a promising photocatalyst for environmental remediation: a study on the importance of hybridization approach. *J Environ Manage*. 2020;255:109936.

doi: 10.1016/j.jenvman.2019.109936

51. Gao KX, Hou LA, An XQ, Huang DD, Yang Y. BiOBr/MXene/g-C3N4 Z-scheme heterostructure photocatalysts mediated by oxygen vacancies and MXene quantum dots for tetracycline degradation: process, mechanism and toxicity analysis. *Appl Catal B Environ*. 2023;323:122150.

doi: 10.1016/j.apcatb.2022.122150

52. Liang Y, Xu WC, Fang JZ, *et al*. Highly dispersed bismuth oxide quantum dots/graphite carbon nitride nanosheets

heterojunctions for visible light photocatalytic redox degradation of environmental pollutants. *Appl Catal B Environ*. 2021;295:120279.

doi: 10.1016/j.apcatb.2021.120279

53. Jiang YN, Gao BY, Wang ZJ, *et al*. Efficient wastewater disinfection by raised 1O2 yield through enhanced electron transfer and intersystem crossing via photocatalysis of peroxymonosulfate with CuS quantum dots modified MIL-101(Fe). *Water Res*. 2023;229:119489.

doi: 10.1016/j.watres.2022.119489

54. Wang FL, Chen P, Feng YP, *et al*. Facile synthesis of N-doped carbon dots/g-C3N4 photocatalyst with enhanced visible-light photocatalytic activity for the degradation of indomethacin. *Appl Catal B Environ*. 2017;207:103-113.

doi: 10.1016/j.apcatb.2017.02.024

55. Tian J, Liu RY, Liu Z, Yu CL, Liu MC. Boosting the photocatalytic performance of Ag2CO3 crystals in phenol degradation via coupling with trace N-CQDs. *Chin Catal*. 2017;38(12):1999-2008.

doi: 10.1016/S1872-2067(17)62926-7

56. Li WX, Wang ZZ, Li Y, Ghasemi JB, Li J, Zhang GK. Visible-NIR light-responsive 0D/2D CQDs/Sb2WO6 nanosheets with enhanced photocatalytic degradation performance of RhB: unveiling the dual roles of CQDs and mechanism study. *J Hazard Mater*. 2022;424:127595.

doi: 10.1016/j.jhazmat.2021.127595

57. Ren HT, Qi F, Labidi A, *et al*. Chemically bonded carbon quantum dots/Bi2WO6 S-scheme heterojunction for boosted photocatalytic antibiotic degradation: interfacial engineering and mechanism insight. *Appl Catal B Environ*. 2023;330:122587.

doi: 10.1016/j.apcatb.2023.122587

58. Chu WH, Wang WM, Deng Y, Peng C. Photosynthesis of hydrogen peroxide in water: a promising on-site strategy for water remediation. *Environ Sci Water Res Technol*. 2022;8(12).

doi: 10.1039/d2ew00504b

59. Chen Z, Yao DC, Chu CC, Mao S. Photocatalytic H2O2 production systems: design strategies and environmental applications. *Chem Eng J*. 2023;451:138489.

doi: 10.1016/j.cej.2022.138489

60. Shi WL, Sun W, Liu YN, *et al*. A self-sufficient photo-Fenton system with coupling in-situ production H2O2 of ultrathin porous g-C3N4 nanosheets and amorphous FeOOH quantum dots. *J Hazard Mater*. 2022;436:129141.

doi: 10.1016/j.jhazmat.2022.129141

61. Zheng LH, Su HR, Zhang JZ, *et al*. Highly selective photocatalytic production of H2O2 on sulfur and nitrogen co-doped graphene quantum dots tuned TiO2. *Appl Catal B Environ*. 2018;239:475-484.

doi: 10.1016/j.apcatb.2018.08.031

62. Thomas N, Dionysiou DD, Pillai SC. Heterogeneous Fenton catalysts: a review of recent advances. *J Hazard Mater*. 2021;404:124082.

doi: 10.1016/j.jhazmat.2020.124082

63. Zhang MM, Lai C, Li BS, *et al*. Unravelling the role of dual quantum dots cocatalyst in 0D/2D heterojunction photocatalyst for promoting photocatalytic organic pollutant degradation. *Chem Eng J*. 2020;396:125343.

doi: 10.1016/j.cej.2020.125343

64. Ma RY, Wang L, Wang H, *et al*. Solid acids accelerate the photocatalytic hydrogen peroxide synthesis over a hybrid catalyst of titania nanotube with carbon dot. *Appl Catal B Environ*. 2019;244:594-603.

doi: 10.1016/j.apcatb.2018.11.087